Effect of Strain Rate and Temperature on Mechanical Properties and Fracture Mechanism of the Dispersion Strengthened Al-12Al_4C_3 System

Oksana Velgosová[1*], Michal Besterci[2], Pritt Kulu[3]

[1]*Technical University Faculty of Metallurgy, Department of Non-ferrous Materials and Waste Treatment, Letná 9/A, Košice 04200, Slovakia*
[2]*Institute of Materials Research, Slovak Academy of Sciences, Watsonova 47, Košice 043 53, Slovakia*
[3]*Tallin University of Technology, Etritajate tee 5, 19086 Tallinn, Estonia*

(Received January 21, 2005: final form February 22, 2005.)

ABSTRACT

The change in fracture for the Al-12Al_4C_3 system has been investigated at temperatures from 293 to 673 K. Under strain rates from $\dot{\varepsilon} = 2.5 \cdot 10^{-5}$ to $\dot{\varepsilon} = 10^{-1}$ s^{-1}. During tensile testing at room temperature, the strain was controlled by dislocation movement and reactions. The first part of the strain was characterized by work hardening expressed by the exponent "n" and the second part was expressed by the local strain in the neck. At high temperatures presently investigated the principal mechanism for originating the strain is attributed to the dynamic recovery process. The effect of strain rate on facture was also analysed.

Keywords: Dispersion strengthened materials; Fracture mechanism; SEM analysis

1. INTRODUCTION

The dispersion strengthened alloys Al-Al_4C_3 prepared by mechanical alloying using powder metallurgy are promising structural materials enabling significant weight reduction for use of aircraft, automobile and materials at elevated temperatures /1-3/. We have described /4/ the optimised condition for producing composite materials by mechanical alloying and their mechanical properties including plasticity at elevated temperatures were presented in /5/. In /6/, the high temperature stability of this alloy was described for long time exposition. In /7-8/, the microstructure change was examined after deformation at elevated temperatures and the fracture mechanism in creep was also studied. The model of "*in-situ*" fracture mechanism for these materials was described /9,10/. It should be mentioned that the kinetics and mechanism of superplastic deformation of various Al alloys are given in many works /11-16/.

The purpose of this work is to present the fracture at different strain rates and temperature for the Al-12Al_4C_3 system. Temperatures and strain rates are from 293 to 673 K and from $\dot{\varepsilon} = 2.5 \cdot 10^{-5}$ to $\dot{\varepsilon} = 10^{-1}$ s^{-1}, respectively. Considering the results reported in /17/ and the strain induced coefficient m ranging from 0.03 to 0.06, this work covers the strain rates from creep to the activation of superplastic behavior.

2. EXPERIMENTAL MATERIAL AND METHODS

The Al-Al_4C_3 composite dispersion strengthened by 12 vol.% of Al_4C_3, was prepared by mechanical

*Corresponding author. E-mail: oksana.velgosova@tuke.sk, Fax number: (+42195) 633 70 48

alloying. The Al powder, grain size under 100 μm, with 1% of KS 2.5 graphite was milling for 90 minutes. Granulate was compacted under the pressure of 600 MPa and annealed at 823 K with a 94% reduction.

The dispersed particles are oriented in layers in the direction of extrusion. The effective size of the particles was found to be 25 x 85 nm, as shown in Fig. 1. There

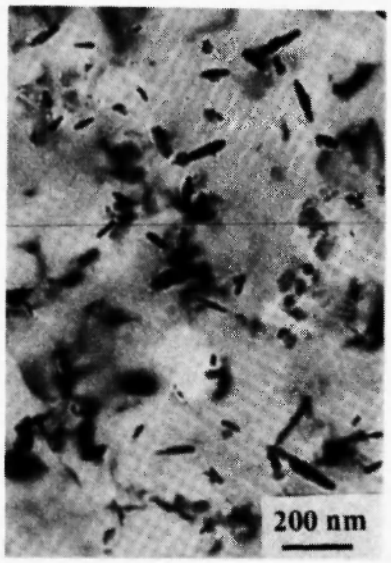

Fig. 1: Effective size of Al_4C_3 particles on the foil.

were also larger dispersed particles and their distribution was estimated to be from 85 nm to 1 μm in size, making up about 30% of dispersoid amount, observed by Scanning Electron Microscopy (SEM) and optical metallography. The Al_4C_3 and Al_2O_3 particles are located in the grain boundaries as well as inside the Al grains. The observed microstructure is fine, even, with grains less than 1 μm, elongated in the direction of extrusion as shown in Fig. 2.

Test pieces of 3 mm in diameter and 15 mm gauge length were machined for tensile test. They were positioned in longitudinal direction, in the direction of extrusion. For the evaluation of strain and fracture mechanisms, SEM observation was made for the fracture surfaces.

3. RESULT AND DISCUSSION

Figure 3 shows the yield strength, $R_{p0.2}$, and the

Fig. 2: The grain size of Al matrix on the foil.

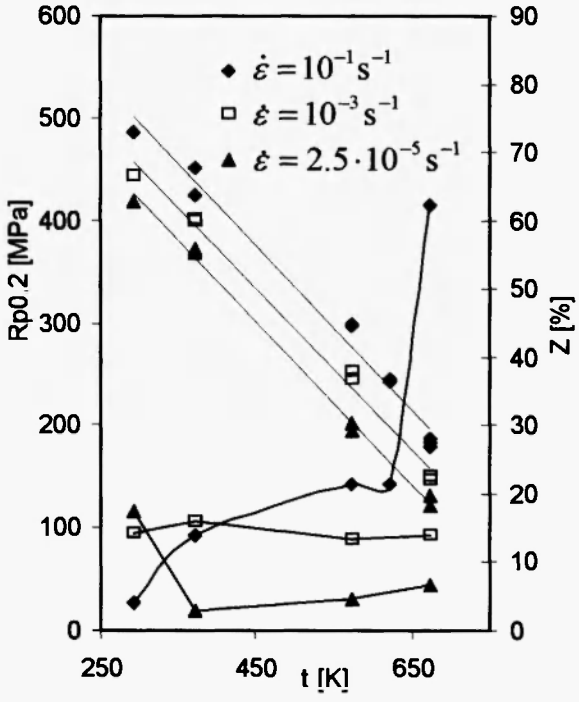

Fig. 3: Influence of temperature and strain rate on yield strength $R_{p0.2}$ and reduction of area Z.

reduction of area, Z, as a function of temperature. The results with strain rates applied are also included in this figure. The results with strain rate of $\dot{\varepsilon}=10^{-1}$ s^{-1} at 673 K indicate a rapid increase in the value of Z. However,

no substantial change is detected in the value of yield strength. It may be worthy of note in Fig. 4 that this is supported by the results obtained for tensile strength, Rm, and elongation, A_5.

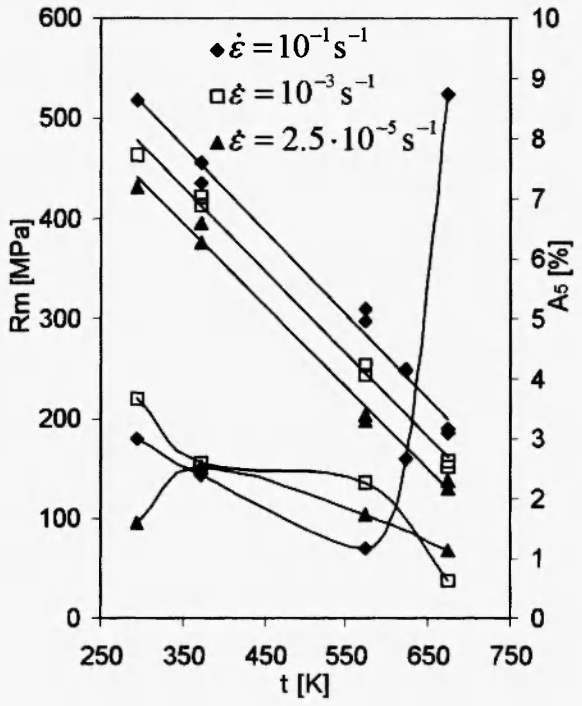

Fig. 4: Influence of temperature and strain rate on tensile strength Rm and elongation A_5.

Figure 5 shows the fracture surface of the sample loaded with high strain rate of $\dot{\varepsilon} = 10^{-1}\ s^{-1}$ at 293 K. On the other hand, the result for the sample with low strain rate of $\dot{\varepsilon} = 2.5 \cdot 10^{-5}\ s^{-1}$ is given in Fig. 6. There are no significant differences in these two results. It is also noted that these two samples are ductile and transcrystalline fracture with dimples. The dimples are found shallow with their typical dimension of 0.45 μm.

Fracture surfaces fractured under strain rate of $\dot{\varepsilon} = 2.5 \cdot 10^{-5}\ s^{-1}$ at 573 K show the underdeveloped intercrystalline facets. They are underdeveloped because the so-called ductile fracture takes place at the end of fracture. Under strain rate of $\dot{\varepsilon} = 10^{-1}\ s^{-1}$, on the other hand, the fracture is considered to be transcrystalline with dimples. The dimples are deeper and larger than is the case at 293 K. The characteristic dimple diameter is around 0.6 μm.

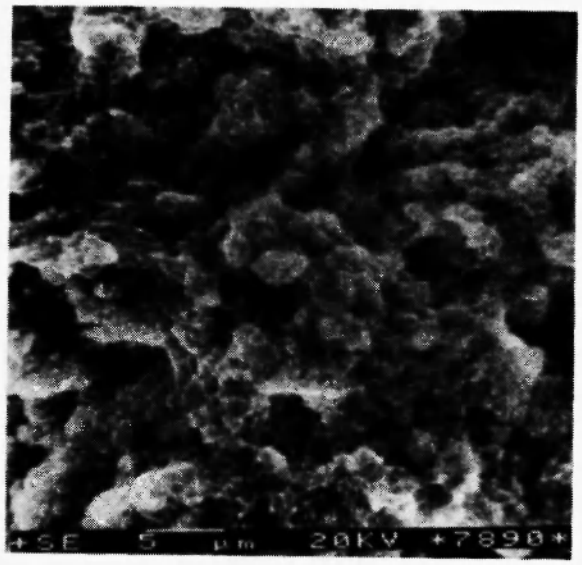

Fig. 5: Transcrystalline fracture surface obtained with strain rate of $\dot{\varepsilon} = 10^{-1}\ s^{-1}$ at 293 K.

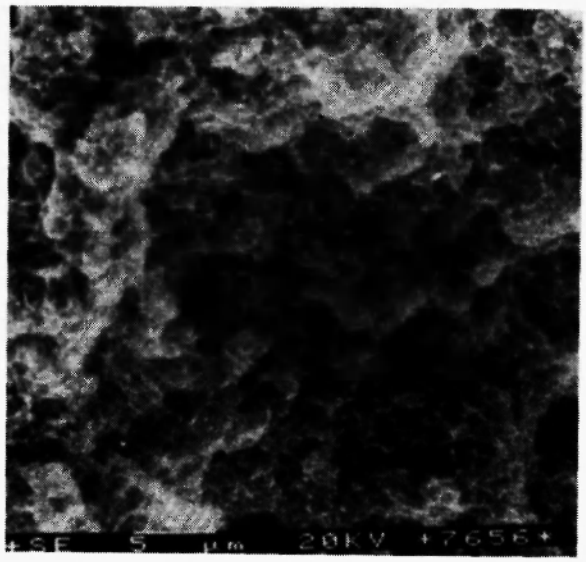

Fig. 6: Transcrystalline fracture surface obtained with strain rate of $\dot{\varepsilon} = 2.5 \cdot 10^{-5}\ s^{-1}$ at 293 K.

Under low strain rate of $\dot{\varepsilon} = 2.5 \cdot 10^{-5}\ s^{-1}$ at 673 K, the fracture is found to take place in the reduction of area Z=8%. Typical micro facets of the fracture are given in Fig. 7. As discussed for metallic materials, the developed intercrystalline facets are present, with dimensions corresponding to the fine grain size, and great angle disorientation. There are small parts of

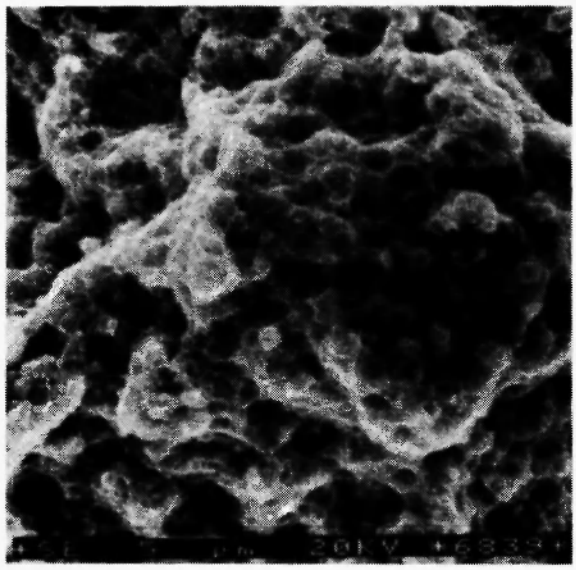

Fig. 7: Intercrystalline fracture surface obtained with strain rate of $\dot{\varepsilon} = 2.5 \cdot 10^{5}\ s^{-1}$ at 673 K.

fracture showing crests of ductile facets. Under strain rate of $\dot{\varepsilon} = 10^{-1}\ s^{-1}$ the fracture is ended at the reduction of area Z=64%, where the fracture is considered to be ductile transcrystalline with developed deep dimples as shown in Fig.8. The characteristic dimple dimension is estimated to be 0.65 μm.

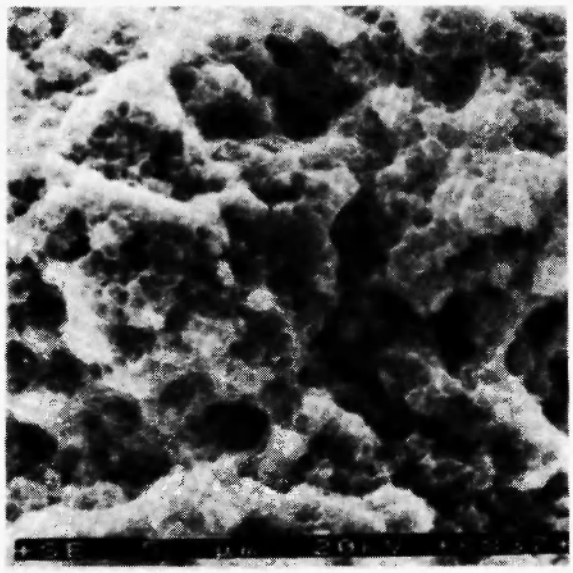

Fig. 8: Transcrystalline fracture surface obtained with strain rate of $\dot{\varepsilon} = 10^{-1}\ s^{-1}$ at 673 K.

The temperature dependence of the middle dimples diameter is shown in Fig. 9 using the case under strain rate $\dot{\varepsilon} = 10^{-1}\ s^{-1}$. The fracture under strain rate $\dot{\varepsilon} = 2.5 \cdot 10^{-5}\ s^{-1}$ at 673 K has been considered intercrystalline fracture, by finding the result of damage to grain boundaries formed by interactions of dislocations with dispersed particles on grain boundaries. However, the fine particles on grain boundaries are important for diffusion creep and strength properties of dispersion strengthened system at high temperatures. Transcrystalline fractures under high strain rates ($\dot{\varepsilon} = 10^{-1}\ s^{-1}$) show a remarkable recovery in the plateau part of the stress-strain curve and this is attributed to the dynamic polygonisation, resulting in the equilibrium of strengthening and weakening. The fracture is caused by voids occurring at the interfaces dispersoid-matrix first on larger particles, after a great amount of strain. The voids are growing and coalesce into dimples of the transcrystalline fracture.

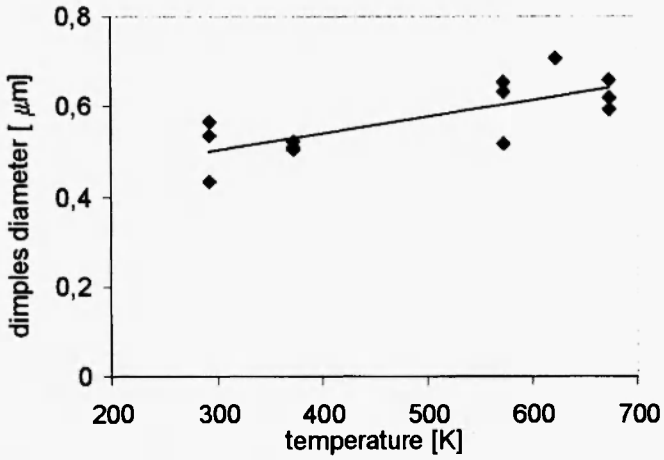

Fig. 9: The middle dimple diameter as a function of temperature using the case with strain rate of $\dot{\varepsilon} = 10^{-1}\ s^{-1}$

4. CONCLUSION

The change in fracture for the Al-12Al_4C_3 system has been investigated at temperatures from 293 to 673 K and with strain rates from $\dot{\varepsilon} = 2.5 \cdot 10^{-5}$ to $\dot{\varepsilon} = 10^{-1}\ s^{-1}$. The results are summarized as follows.

1. At 293 K, during tensile testing under strain rates

presently tested, the strain is at first controlled by work hardening, expressed by the exponent *n*. In the next stage, the deformation is, more or less, affected by local straining and forming the neck.

2. There is a marked decrease of plastic properties under strain rate of $\dot{\varepsilon} = 2.5 \cdot 10^{-5}$ s^{-1} with increasing temperature. The results are considered relevant to changes in micromechanism of deformation and fracture. At 293 K, fracture surface shows the transition from ductile fracture with dimples to intercrystalline fracture, suggesting the exhausted grain boundary plasticity with increasing temperature.
3. In the results under strain rate of $\dot{\varepsilon} = 10^{-1}$ s^{-1} at 673 K, the first part of the strain characterized by work hardening was found to be very short. Then, the stress quickly reached the maximum. In this stage, the thermally and mechanically activated dynamic recovery is quite likely to take place where the strain is uniform all over the body of the test piece. The fracture process indicates an increase of cavities and it is described by transcrystalline fracture with deep dimples.

ACKNOWLEDGEMENT

This work has been supported by grant 2/5142/25.

REFERENCES

1. G. Jangg, F. Kutner and G. Korb, *Aluminium*, **51**, 641 (1975).
2. G. Jangg, G. Korb and F. Kutner, in: *6. Internationale Leichtmetalltagung, Aluminiuum Verlag*, Dusseldorf, 1977, p. 23.
3. G. Korb, G. Jangg and F. Kutner, *Draht*, **5**, 1 (1979).
4. M. Slesár, G. Jangg, M. Besterci and J. Durišin, in: *Internationale Leichtmetalltagung*, Leoben-Wien, 1981, p.238.
5. M. Slesár, M. Besterci, G. Jangg, M. Miškovičová and K. Pelikan *Z. Metallkunde*, **Bd.79 (H1)**, 56 (1988).
6. M. Slesár, G. Jangg, M. Besterci, J. Durišin and M. Orolínová *Z. Metallknde*, **Bd.80 (H11)**, 817 (1989).
7. M. Slesár, G. Jangg, J. Durišin, M. Besterci and M. Orolínová, *Mat-Wiss. U. Werkstoffmechanik*, **23**, 13 (1992).
8. M. Slesár, M. Besterci and G. Jangg, *Z. Metallkunde*, **Bd.83 (H3)**, 183 (1992).
9. M. Besterci and J. Ivan, *J. of Mat. Sci. Letters*, **15**, 2071 (1996).
10. M. Besterci, J. Ivan, O. Velgosová and L. Pešek, *Kovové Mat.* **39** (6), 361 (2001).
11. R.S. Mishra and A.K. Mukherjee, *Mater. Sci. Eng.* **A234-A236**, 1023 (1997).
12. R.S. Mishra, T.R. Bieler and A.K. Mukherjee, *Scripta Metall.* **26**, 1605 (1992).
13. T.R. Bieler and A.K. Mukherjee, *Materials Trans. JIM* **32**, 1149 (1991).
14. T.G. Nieh, J. Wadsworth and T. Imai, *Scripta Metall.* **26**, 703 (1992).
15. M. Sakai and H. Muto, *Scripta Mater.* **38**, 909 (1998).
16. A. Urena, J.M. Gomez de Salazar, J. Qiunones and J.J. Martín, *Scripta Mater.* **34** (4), 617 (1996).
17. T. R. Bieler, T. G. Nieh, J. Wadsworth and A. Mukherjee, *Scripta Metallurgica et Materialia*, **22**, 81 (1988).